AD-A126 870 RETROGRADE AMNESIA IN RATS PRODUCED BY ELECTRON BEAM EXPOSURE(U) SCHOOL OF AEROSPACE MEDICINE BROOKS AFB TX T G WHEELER ET AL. FEB 83 SAM-TR-83-3 1/1

UNCLASSIFIED F/G 5/10 • NL

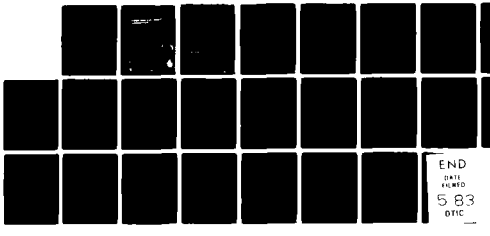

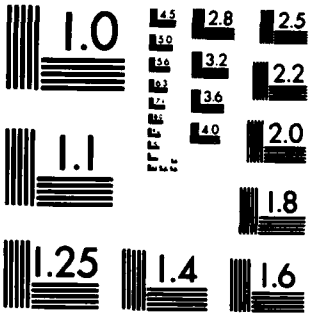

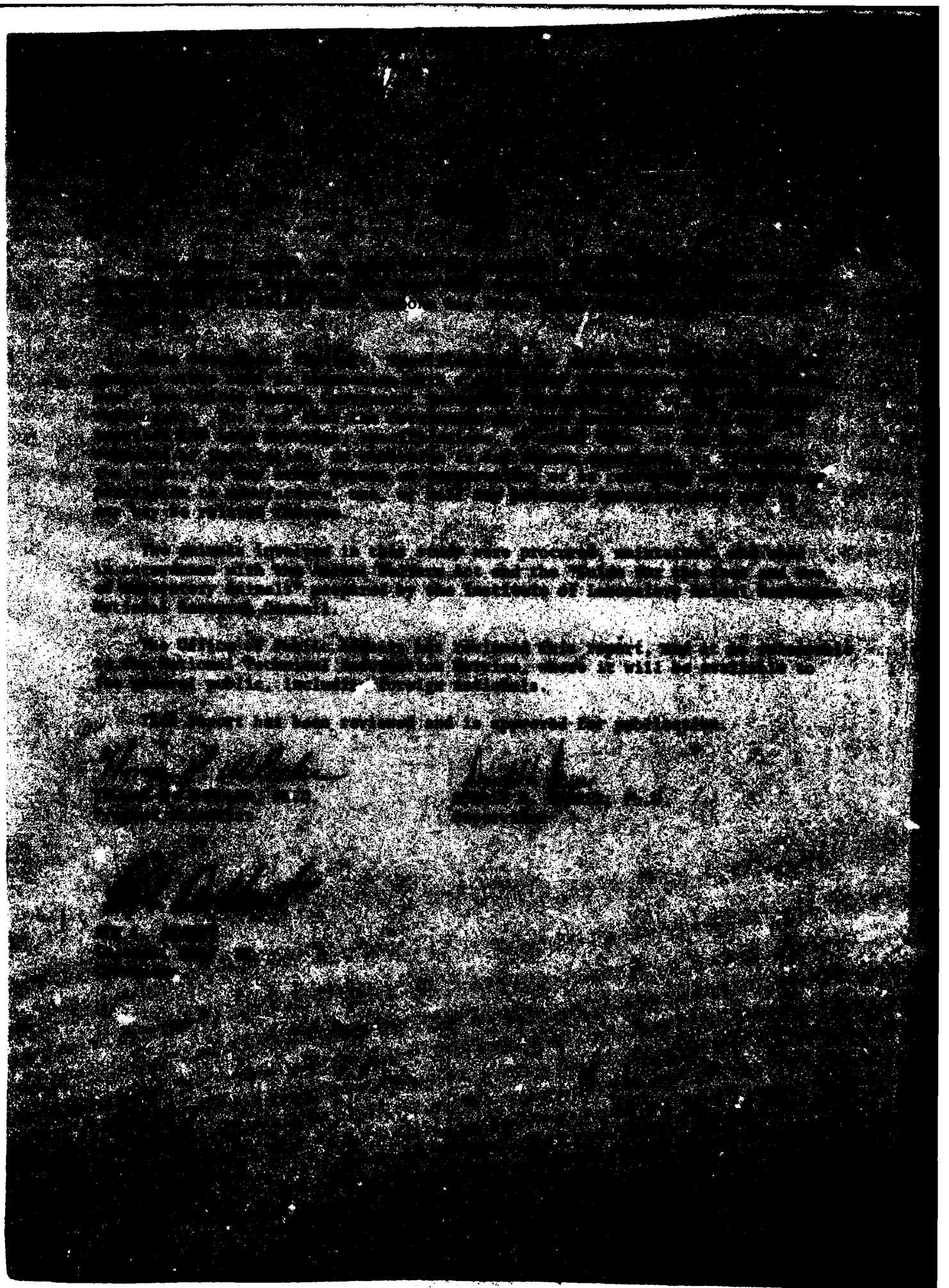

UNCLASSIFIED

SECURITY CLASSIFICATION OF THIS PAGE (When Data Entered)

REPORT DOCUMENTATION PAGE		READ INSTRUCTIONS BEFORE COMPLETING FORM
1. REPORT NUMBER SAM TR- 83-3	2. GOVT ACCESSION NO. AD-A126879	3. RECIPIENT'S CATALOG NUMBER
4. TITLE (and Subtitle) RETROGRADE AMNESIA, IN RATS, PRODUCED BY ELECTRON BEAM EXPOSURE		5. TYPE OF REPORT & PERIOD COVERED Final Report July 1982 - September 1982 6. PERFORMING ORG. REPORT NUMBER
7. AUTHOR(s) Thomas G. Wheeler, Ph.D. Kenneth A. Hardy, M.S. Dennis W. Blick, Ph.D. (Systems Research Labs., Inc.)*		8. CONTRACT OR GRANT NUMBER(s)
9. PERFORMING ORGANIZATION NAME AND ADDRESS USAF School of Aerospace Medicine (RZW) Aerospace Medical Division (AFSC) Brooks Air Force Base, Texas 78235		10. PROGRAM ELEMENT, PROJECT, TASK AREA & WORK UNIT NUMBERS 62202F 7757-05-55
11. CONTROLLING OFFICE NAME AND ADDRESS USAF School of Aerospace Medicine (RZW) Aerospace Medical Division (AFSC) Brooks Air Force Base, Texas 78235		12. REPORT DATE February 1983 13. NUMBER OF PAGES 30
14. MONITORING AGENCY NAME & ADDRESS(if different from Controlling Office)		15. SECURITY CLASS. (of this report) UNCLASSIFIED 15a. DECLASSIFICATION/DOWNGRADING SCHEDULE

16. DISTRIBUTION STATEMENT (of this Report)

Approved for public release; distribution unlimited.

17. DISTRIBUTION STATEMENT (of the abstract entered in Block 20, if different from Report)

18. SUPPLEMENTARY NOTES

* 2800 Indian Ripple Road, Dayton, Ohio 45440

19. KEY WORDS (Continue on reverse side if necessary and identify by block number)

Amnesia
Electron beam
Performance decrement

20. ABSTRACT (Continue on reverse side if necessary and identify by block number)

That electron beam exposure produces retrograde amnesia (RA) has been demonstrated. RA production was evaluated using a single trial avoidance task across a 10^4 dose range for 10 μs, 1 μs, and 0.1 μs pulsed exposures. The dose-response curve obtained at each pulse duration showed significant RA production. The most effective dose range was 0.1-10 rads at a dose rate of 10^6 rad/sec. Our conclusion was that the RA effect might be due to sensory system activation which provided a novel stimulus that masked previous stimuli (produced RA).

DD FORM 1 JAN 73 1473 EDITION OF 1 NOV 65 IS OBSOLETE

UNCLASSIFIED

SECURITY CLASSIFICATION OF THIS PAGE (When Data Entered)

C O N T E N T S

Page

INTRODUCTION 3

METHODS 3

Single Trial Avoidance 3
Learning Ability 4
Index of General Stress 4
Experimental Design 4

DOSIMETRY 5

RESULTS 5
Learning Ability 9
Stress 10

DISCUSSION 11

REFERENCES 12

APPENDIX A: Dosimetry Measurements at the White Sands Missile Range Linear Electron Accelerator Facility, 3 May 1982 and 2 July 1982.. 16

Introduction 16
Experimental Procedures 16
Experimental Dosimetry Results 20
Discussion 24
References 25

APPENDIX B: Statistical analysis 29

Methods and Results 29
References 29

Illustrations

Figure No.

1. Mean latency difference (T' - T) between treatment and test trials as a function of dose and exposure pulse width 8

2. Mean latency difference (T' - T) as a function of exposure dose rate 9

A-1. Diode response at 1.0 μs pulse width, 100 rad (Si) per pulse (computer printout) 18

A-2. Dosimeter, phantom, and chamber exposure configurations (overhead view) 19

CONTENTS (Cont'd.)

Figure No.		Page
A-3.	Beam map: Front of chamber at 10-μs pulse width, 500 rads/pulse, one pulse	23
A-4.	Beam map: Front of chamber at 20 ns, 1 rad/pulse, 100 pulses	26
A-5.	Depth dose distribution measured in Plexiglas phantom at 10-μs pulse width, 1 rad/pulse, 100 pulses	27

Table No.		
1.	Exposure conditions of test groups	5
2.	Latency data (T' - T) from all test groups in terms of median, range, mean, standard deviation, and standard error of the mean	6
3.	The mean number of avoidances on two-way avoidance learning task..	10
A-1.	Dosimetric results of phantom TLD measurements in rads tissue on White Sands Missile Range Linear Electron Accelerator, 3 May 1982 and 2 July 1982	21
A-2.	Dosimetric results of map and depth dose TLD measurements in rads tissue	22
A-3.	Dose per pulse, White Sands Missile Range diode in rads silicon vs. USAFSAM TLDs in rad tissue	28
B-1.	Analyses of variance and summary statistics for multiple linear regression to predict mean (T' - T) difference from $\log_{10}$ (dose) and ($\log_{10}$ (dose) · ($\log_{10}$ (dose rate))	30
B-2.	Cell values are group numbers, observed cell means, and predicted values (=14.52 - 36.75 $\log_{10}$ (dose) + 6.13 $\log_{10}$ (dose) $\log_{10}$ (dose rate) · $\log_{10}$ dose rate	30

ACKNOWLEDGMENTS

Our thanks are extended to the many individuals who have provided support in this project. Especial appreciation is expressed to the professionals at: the Primate Research Center (Holloman AFB), for animal care and general support; and the Veterinary Sciences Division and Systems Research Laboratories (Brooks AFB), for performing the ulcer evaluations and shuttle avoidance tests. We also thank: Master Sergeant Mark Frechette, for technical assistance; Senior Airman Karen Page, for professional assistance in performing the experimental trials; and Mrs. Mary Nash, for administrative assistance.

RETROGRADE AMNESIA, IN RATS, PRODUCED BY ELECTRON BEAM EXPOSURE

INTRODUCTION

Retrograde amnesia (RA) is a form of memory loss characterized by inability to recall events preceding the trauma or stimulus that produced the memory deficit. Many stimuli have been demonstrated to be effective in producing RA: e.g., electroconvulsive shock (ECS) (14,19); hypoxia (9); and drugs (3,7). Preliminary studies have shown that a sublethal exposure to an electron beam also produces RA (16). This result was unexpected; no previous ionizing radiation study had shown RA at such low levels.

What, then, are the causal parameters--and by what mechanism could electron beam exposure produce RA? The present study was designed to determine: (a) if the extent of RA production varied as a function of dose and dose rate; (b) if electron beam exposure affected learning ability; and (c) if electron beam exposure produced a general physiological stress response. These data provide some indication of the potential hazards of electron beam exposure, and suggest a mechanism of RA production.

METHODS

The effects of electron beam exposure were examined by employing three measures: (a) a single trial avoidance task (for RA production); (b) a two-way shuttle avoidance task (learning ability); and (c) the production of stomach ulcers (index of general stress). Each of these tests is outlined in the following sections of this report.

Single Trial Avoidance

The task and apparatus have previously been described in detail (24). Briefly, the task was a single-trial avoidance paradigm. The test procedure began when the animal was placed in a small aversive chamber. After a 90-sec adaptation period, a door opened that provided access to a large, dark "preferred" chamber. The time required for the animal to leave the illuminated "aversive" chamber and enter the preferred chamber was the dependent variable (denoted T). Once inside the preferred chamber, a foot shock of 85 V (peak to peak) was delivered to the animal for 1 sec. At 1 sec after the termination of the shock, the linear electron accelerator (LINAC) was pulsed, thus exposing the animal to the electron beam. The animal was then returned to its home cage. A second trial on the same task was run 2 hr postexposure. The second trial consisted of placing the animal in the aversive chamber, and of monitoring the time (T') required for the animal to enter the preferred chamber. No shock or LINAC pulse was presented on the second trial.

If the animal recalled the shock treatment on the first trial, the values of T' (second trial latency) would be large. If the electron beam exposure

interfered with the animal's ability to recall the shock, T' would be greatly reduced as compared with the sham controls. The operational definition of RA for this study was the value of T' - T, between the limits of complete recall of the shock (a shock, no exposure condition), and no recall of a shock (no shock presented). The upper and lower limits of T' - T have been evaluated by employing a sham exposure group and additional control groups (Table 1). The data of the control groups provided reference points to which could be compared the data from test groups receiving exposures at various dose rates and total doses. One of the additional control groups was exposed to the electron beam before undergoing the normal treatment (just outlined) in order for us to determine if preexposure to an electron beam affected subsequent RA production.

Learning Ability

The morning after each test day on the LINAC at White Sands, N.M., animals from Groups 1, 3, and 5 (Table 1) were air freighted to Brooks Air Force Base, Tex. At 48 hr postexposure, these animals were tested on a two-way shuttle avoidance task. Details of the test procedures have already been presented (15). The number of avoidances within sixty trials was used as a measure of learning ability.

Index of General Stress

Immediately after the two-way avoidance test, the animals were sacrificed (halothane) and necropsy was performed by personnel in the Veterinary Sciences Division (VSP), to determine the number and size of stomach ulcers as a measure of general physiologic stress (18). We had no reason to believe that electron beam exposure would produce stress at the levels used, but we knew that stress affected learning ability (15). Therefore, knowing the degree of stress (from shipping, exposure, etc.) was important in order to interpret the learning data.

Experimental Design

Two hundred and ten Sprague-Dawley male rats (240 gm $\pm$ 20 gm) were purchased and individually housed under a 12-hr-on and 12-hr-off light cycle, with free access to food and water, for 2 weeks preexposures. The animals were housed at the Primate Research Center, Holloman AFB, N.M. Twenty-four hours before each treatment day, 50 animals were ear-tagged and transported to the White Sands Missile Range (WSMR) [LINAC Facility]. The experiments were run from 0900 to 1700 hr. At 0700 on the morning after exposures and single-trial testing, animals from Groups 1, 3, and 5 were sent to Brooks AFB for evaluation of learning ability and degree of stress present. Animals, naive to all tests and procedures, were randomly assigned to the experimental groups listed in Table 1.

TABLE 1. EXPOSURE CONDITIONS OF TEST GROUPS

A. Primary Experimental Matrix

		Dose (rads)				
		Sham	0.1	1.0	10	100
Pulse width	10 μs	1[a]	2	3	4	5
	1.0 μs		6	7	8	9
	0.1 μs		10	11	12	b

B. Additional Control Groups [c]

No shock + no exposure	No shock + 10-rad exposure	No shock + 100-rad exposure	Preexposure to 10 rad, then shock + 10-rad exposure
13	14	15	16

[a]Group numbers (Group 1, N = 20; Groups 2 - 16, N = 13)

[b]Outside LINAC operating range

[c]The exposure pulse width for Groups 14, 15, and 16 was 10 μs.

DOSIMETRY

Dosimetry was performed in two ways: First, field maps were made of the beam to insure that the field was uniform across the exposure chamber, and phantoms were used to evaluate midline dose. Second, a calibrated silicon diode was placed in the beam path, and a readout of each animal's exposure was obtained. The average of the individual exposures for each group has been listed in Table 2 as mean dose with standard error of the mean. A complete description of the dosimetry is presented in Appendix A.

RESULTS

The results of the single trial avoidance experiment are presented in Figures 1 and 2 and Table 2. The results of the learning and ulcer evaluations follow the RA data.

TABLE 2. LATENCY DATA (T' - T) FROM ALL TEST GROUPS IN TERMS OF MEDIAN, RANGE, MEAN, STANDARD DEVIATION (SD), AND STANDARD ERROR OF THE MEAN (SEM)

A. Primary Experimental Matrix

Pulse width		Dose (rads) Sham	0.1	1.0	10	100
	Group No.		2	3	4	5
	Median		17.2	3.7	3.5	41.0
	Range		-2.7 to 94.0	-4.2 to 95.1	-13.6 to 21.8	-9.0 to 96.4
10 μs	Mean		27.7	21.2	4.1	40.8
	SD		31.7	37.7	10.3	36.1
	SEM		8.8	10.4	2.9	10.0
	Mean Dose(rads)		0.083 ±0.039	1.20 ±0.11	10.8 ±1.2	108 ±3.8

Pulse width						
	Group No.	1	6	7	8	9
	Median	22.0	7.8	0.4	7.5	10.6
	Range	-0.1 to 97.8	-1.5 to 94.6	-3.1 to 15.3	-2.3 to 71.1	-3.6 to 95.6
1 μs	Mean	39.3	22.5	2.9	23.0	31.7
	SD	34.9	29.9	5.9	25.2	37.9
	SEM	7.8	8.3	1.6	7.0	10.5
	Mean Dose(rads)		0.091 ±0.004	1.36 ±0.14	11.8 ± 0.87	106 ± 5.1

TABLE 2 (Cont'd.)

Pulse width		Dose (rads) 0.1	1.0	10
	Group No.	10	11	12
	Median	4.3	5.5	13.4
	Range	-6.9 to 94.5	-10.6 to 97.9	-1.9 to 97.1
100 ns	Mean	14.3	20.6	24.5
	SD	27.6	35.4	30.3
	SEM	7.7	9.8	8.4
	Mean Dose (rads)	0.17 ±0.005	1.25 ±0.10	11.2 ±0.72

B. Additional Control Groups

	No shock + no exposure	No shock + 10 rad	No shock + 100 rad	Preexposure to 10 rad, then shock + 10 rad
		(rads)		
Group No.	13	14	15	16
Median	-0.3	-1.1	-0.9	43.2
Range	-2.5 to 1.5	-5.8 to 11.9	-3.8 to 4.0	-0.2 to 96.5
Mean	-0.7	-1.0	-0.8	46.8
SD	1.2	4.9	2.4	40.1
SEM	0.3	1.4	0.7	11.5
Mean Dose (rads)		10.4 ±0.2	107 ±3.9	10.2 ±0.3

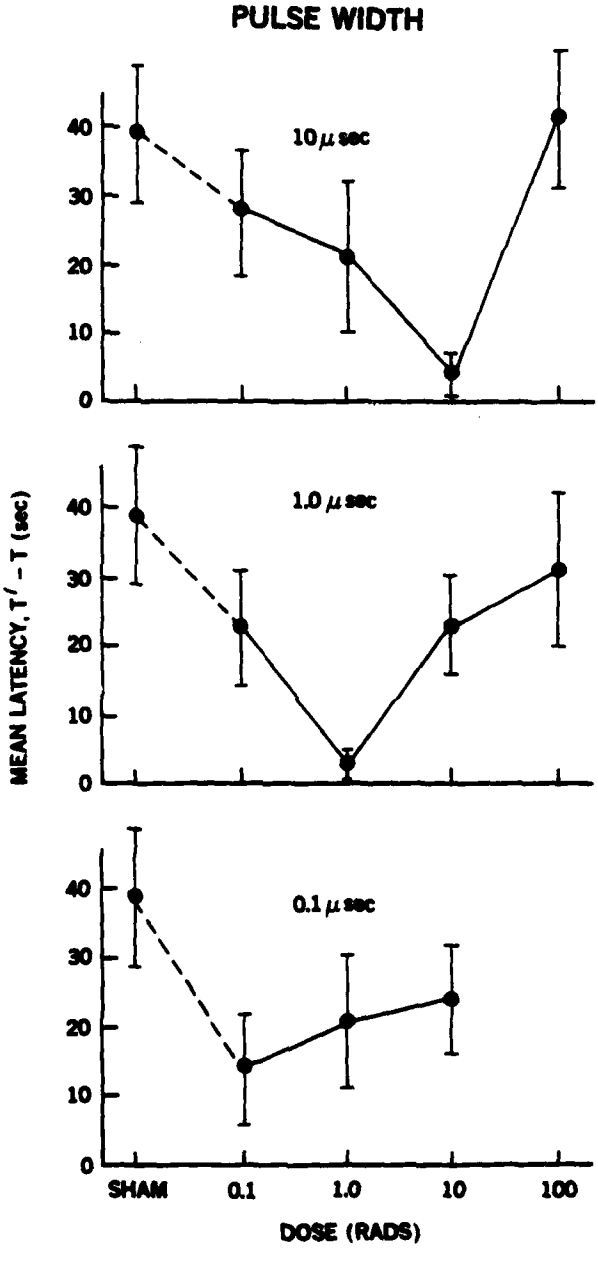

Figure 1. Mean latency difference (T' - T) between treatment and test trials as a function of dose and exposure pulse width.

The shift in effective dose across pulse widths (Fig. 1) suggests that dose rate may be another important stimulus parameter. The data from the experimental matrix (Table 1, Section A) were, therefore, grouped by dose rate and averaged (Fig. 2). Averaging the dose rate data across dose, as in Figure 2, should not be construed as meaning that these parameters were mutually exclusive. Indeed, not only were dose and dose rate shown to be important parameters, but a significant interaction was also observed (Appendix B).

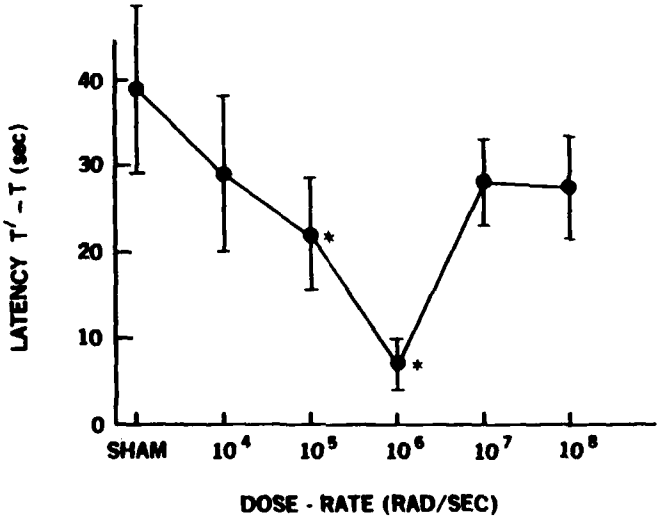

Figure 2. Mean latency difference (T' - T) as a function of exposure dose rate.

A histogram of each group's data indicated that the T - T' distributions differed across test groups. Some distributions were normal, and others approached bimodal. This finding is reflected in the differences between the medians and means listed in Table 2. Statistical evaluations of these data are presented in detail in Appendix B.

Learning Ability

The results of the two-way shuttle avoidance learning task are presented in Table 3.

TABLE 3. THE MEAN NUMBER OF AVOIDANCES ON TWO-WAY AVOIDANCE LEARNING TASK

	Dose (rads)		
	Sham	1 rad	100 rad
Group No.	1	3	5
Mean	35.2	33.2	30.1
SD	19.4	16.2	15.2
SEM	6.9	4.5	4.8

Stress

The veterinarian who examined the animals determined, not knowing the animals' previous treatment, that no ulcers were present in any animal. Also, all animals were reported to be in good health.

These results can be summarized as follows:

1. The most effective dose range for RA production was from 0.1 to 10 rad, with decreasing effectiveness for higher or lower doses (Fig. 1).

2. The most effective dose rate was 10^6 rad/sec with decreasing effectiveness at lower and higher dose rates. Note, in Figure 1, that the lowest point on each curve occurs at 10^6 rad/sec; i.e., minimum for 10 μs pulse was at 10 rads, 10 rad/10 X 10^{-6} sec = 10^6 rad/sec, etc.

3. Exposure to an electron beam at 10 or 100 rads was not aversive to the animal (compare Groups 14 and 15 to Group 13), as indicated by relative latency (T' - T).

4. Preexposure of the animal to a pulsed electron beam eliminated the RA effect (compare Groups 4 and 16).

5. No significant differences in shuttle-box learning ability existed 48 hr postexposure, between the sham, 1-rad, or 100-rad groups (Groups 1, 3, and 5).

6. The total lack of stomach ulcers in Groups 1, 3, and 5 indicates that the animals were not severely stressed by treatments or transportation. This measure could provide no indication of differences in stress levels among groups.

DISCUSSION

Numerous findings in the data can be related to previous reports. The most prominent trend was the low-dose effect: RA was produced at 0.1 rad with a 0.1- μsec pulse exposure. This finding provides some indication of possible mechanisms. Since storage of information (memory) is a central nervous system (CNS) function, any stimulus which disrupts memory must activate the CNS. Activation of the CNS occurs normally via the sensory systems, but can also be achieved by experimental manipulations (e.g., local drug injection, temperature changes, induced current, or ionizing radiation). The most likely mechanisms of CNS activation by electron beam exposure are: (a) direct stimulation of CNS neurons via ionization or induced current; or (b) stimulation of one or more of the sensory systems. Each of these possibilities will be considered in turn.

Direct activation of neurons in the CNS via ionization has been shown to require doses greater than 1000 rad across radiation sources, with larger doses producing larger effects (13). The data reported here indicate RA production at 0.1 rad, the lowest level tested. This low-dose effect argues against ionization as a mechanism of CNS activation.

Current induction via electroconvulsive shock (ECS) is known to produce RA (14,19). However, no data are available on the amount of current at the neural level required to produce RA. Also unknown is whether the secondary or Compton currents produced by electron beam exposure are qualitatively or quantitatively similar to currents produced by ECS. Although direct comparison between ECS and electron beam currents cannot be made, reports indicate that repeated preexposures to ECS are required to reduce the RA effect (12). In contrast, a single preexposure to an electron beam totally eliminates the RA effect, thus suggesting that CNS activation via induced current was probably not the mechanism of RA production.

The low-dose effect strongly suggests sensory activation. Every sensory system studied appears to be sensitive to ionizing radiation, some at very low doses (less than 0.1 rad). The olfactory response threshold to ionizing radiation has been shown to be less than 10 mrad (8). The visual system is sensitive to radiation levels below 0.5 mrad (10,17). Ionizing radiation has been shown to be as efficient as light in producing retinal activity, as monitored by the electroretinogram (1,22,23). Also, sensory systems are primarily sensitive to dose rate, not absolute dose. For the visual system, U-shaped dose-rate response functions (Fig. 2) are commonly observed (11,20,21). The olfactory system is more sensitive to dose rate than total dose for low-level x-ray exposures (5). Therefore, an hypothesis is that an electron beam exposure could have produced RA via activation of one or more of the sensory systems.

Irrespective of how many sensory systems may be involved or the extent of activation of each, exposure would obviously constitute a novel stimulus, particularly since the stimulus was presented in an unfamiliar environment. The "recency theory" appears to apply here. This theory states that, if two or more novel stimuli are sequentially presented, the subject will recall the last stimulus most vividly; i.e., will recall the most recent event (2). In this experiment, two novel stimuli were sequentially presented--a mild shock followed by electron beam exposure. When both stimuli were presented, the animal recalled

the most recent (forgot the former). When the animal was preexposed to the beam, thereby reducing its novelty, the animal again recalled the most recent novel stimulus, the shock.

If electron beam exposure produced a novel stimulus via sensory system activation, then activation by conventional stimuli would reasonably be assumed also to produce RA. This theory was tested by a 10^{-6} sec photoflash in place of electron beam exposure, and RA resulted (24). The same study demonstrated that the extent of RA production was related to photoflash intensity. Also, when the animals were preexposed to a photoflash, the photoflash was no longer an effective amnesiac, just as was the case for electron beam preexposure. The major difference between the photoflash and electron beam RA data was the effect at high doses. The photoflash data showed no indication of reduced effectiveness at the highest intensities used, whereas the RA effect decreased at the higher dose electron beam exposures. At the higher doses, mechanisms other than simple sensory activation were apparently involved. This finding is consistent with the "dual-factor" hypothesis for the effects of small doses of ionizing radiation (4): i.e., the first mechanism (factor) is sensory detection which is dose-rate dependent; and the second factor is a function of ionization due to accumulated doses. Additional biological systems may also be affected at the higher dose levels via ionization or induced current. By whatever mechanisms, CNS activation must have increased as a function of exposure level. The U-shaped dose-response curves (Fig. 1) support this contention. Activation theories, such as the Yerkes-Dodson Law, predict a U-shaped dose-response function: A given task has an optimal amount of CNS activation; a greater or a lesser degree of activation will result in a performance deficit (25). Another interesting project would be to learn which biological systems were activated as a function of exposure level.

Any experiment that utilizes ionizing radiation as a stimulus raises the question of potential biological hazards. Simply stated, we had no indication of harmful effects from the data presented here; i.e., a 100-rad exposure was not aversive, and preexposure eliminated the RA effect. This exposure produced no sign of physiological stress and no learning deficit. However, other amnesiacs have been shown to be harmful if administered repeatedly (6). The major focus of study here was RA production. The extent to which other biological systems may be affected and the effects of electron beam exposure on other CNS functions remain virtually unknown. An interesting area for future research would be the extent of memory loss in relation to exposure levels.

REFERENCES

1. Bachofer, C. S., and S. E. Wittry. Electroretinogram in response to x-ray stimulation. Science 133:642-644 (1961).

2. Baddeley, A. D., and G. J. Hitch. Recency reexamined, pp. 647-667. In S. Dormic (ed.). Attention and performance VI. New York: John Wiley and Sons, 1977.

3. Bartus, R. T. Physostigmine and recent memory: effects in young and aged nonhuman primates. Science 206:1087-1089 (1979).

4. Buchwald, N. A., J. Garcia, B. H. Feder, and and G. Bach-y-Rita. Ionizing radiation as a perceptual and aversive stimulus, pp. 687-699. In T. J. Haley and R. S. Snider (eds.). Response of the nervous system to ionizing radiation. Boston, Mass.: Little Brown and Co., 1964.

5. Cooper, G. P. Receptor origin of the olfactory bulb response to ionizing radiation. Am J Physiol 215:803-806, 1968.

6. Cronholm, B., and L. Molander. Memory disturbances after electroconvulsive therapy: conditions one month after a series of treatments. Acta Psychiatr Scand 40:211-216 (1964).

7. DeWied, D., and B. Bohus. Modulation of memory processes by neuropeptides of hypothalmic-neurohypophyseal origin, pp. 139-149. In M. A. B. Brazier (ed.). Brain mechanisms in memory and learning. New York: Raven Press, 1979.

8. Dinc, H. I., and J. C. Smith. Role of the olfactory bulbs in the detection of ionizing radiation by the rat. Physiology and Behavior 1:139-144 (1966).

9. Flohr, H. Hypoxia-induced retrograde amnesias, pp. 277-291. In M. A. B. Brazier (ed.). Brain mechanisms in memory and learning. New York: Raven Press, 1979.

10. Gurtovoi, G. K., and Ye. O. Burdianskaia. Visual sensations induced by x-irradiation of the eye with doses of the order of one milliroentgen. Biophys (USSR) 4:65-71 (1959).

11. Kelly, D. H. Effects of sharp edges in a flickering field. J Opt Soc Am 49:730-732 (1959).

12. Kesner, R. P., and J. H. McDonough. Diminished amnestic effect of a second electroconvulsive seizure. Exp Neurol 27:527-533 (1970).

13. Kimeldorf, D. J., and E. L. Hunt. Neurophysiological effects of ionizing radiation: the central nervous system, pp. 68-69. In Ionizing radiation: neural function and behavior. New York: Academic Press, 1965.

14. Kopp, R., Z. Bohdanecky, and M. E. Jarvik. Long temporal gradient of retrograde amnesia for a well-discriminated stimulus. Science 153:1547 (1966).

15. Lanum, J., M. E. Campbell, D. W. Blick, T. G. Wheeler, and J. T. Yates. Behavioral and physiological effects of psychological stress in rats. USAFSAM-TR-82-34, Dec 1982.

16. McNulty, P., and V. P. Pease. Retrograde amnesia as a function of high dose rate, low total dose electron beam. Lectures presented at the USAF School of Aerospace Medicine, Weapons Effects Branch, Brooks AFB, Tex., 1981. (Lecturers were faculty members from the Department of Physics, Clarkson College, Potsdam, N. Y.)

17. Pape, R., and J. Zakovsky. Die Roentgen-strahlensensibilität der Retina. Fortschr Gebiete Roentgenstrahlen 80:65-71 (1954).

18. Pare, W. P. Psychological studies of stress ulcer in the rat. Brain Res Bull 5:73-79 (1980).

19. Quartermain, D., R. M. Paolino, and N. E. Miller. A brief temporal gradient of retrograde amnesia independent of situational change. Science 149:1116 (1966).

20. Riedemeister, C., and O. J. Grusser. Flimmerlicht-untersuchungen an der Katzenretina. 1. On-Neurone und on-off Neurone. Fur Biol III:241-253 (1959).

21. Schwarz, F. Uber Die Wirkung von Wechselstrom auf des Schorgan. Z. Sinnesphysiol 67:227-244 (1938).

22. Smith J. C., and D. J. Kimeldorf. The bioelectrical response of the insect eye to beta radiation. J Insec Physiol 10:839-847 (1964).

23. Smith, J. C., and H. L. Taylor. Immediate detection of x-rays by the rhesus monkey. Radiation Research 35:528 (1968).

24. Wheeler, T. G. Amnesia production by visual stimulation. USAFSAM-TR-82-15, Dec 1982.

25. Yerkes, R. M.,and J. D. Dodson. The relation of strength of stimulus to rapidity of habit-formation. J Comp Neurol Psychol 18:459-482(1908).

APPENDIXES:

A. Dosimetry Measurements at the White Sands Missile Range Linear Electron Accelerator Facility, 3 May 1982 and 2 July 1982

B. Statistical Analysis

APPENDIX A:

DOSIMETRY MEASUREMENTS AT THE WHITE SANDS MISSILE RANGE LINAC FACILITY, 3 May 1982 and 2 July 1982

Introduction

This report describes dosimetry performed on the Nuclear Effects Laboratory LINAC (Linear Electron Accelerator) Facility at the White Sands Missile Range (WSMR), N. M., on 3 May 1982 and 2 July 1982. The work was performed in support of USAFSAM/RZ behavioral and bioeffects studies under project 7757-05-55, with Dr. Thomas G. Wheeler as Principal Investigator. The prime objective dosimetrically was to determine the capability of the WSMR LINAC facility to provide single pulse electron beams suitable for the whole body exposure of 200 - 250 g rodents over the pulse width range of 10 ns - 10 μs and a dose range of 1 - 500 rad/pulse. This objective was achieved by dosimetry measurements with thermoluminescent dosimeters (TLDs) exposed in cylindrical water-filled phantoms approximating the size of the animals to be used in the experiment. Phantom exposures were conducted at the following programmed pulse width and dose per pulse combinations:

Pulse width	Dose per pulse
20 ns	1 rad
100 ns	1, 10 rad
1 μs	1, 10, 100 rad
10 μs	1, 10, 100, 500 rad

The phantoms were exposed in an experimental exposure chamber identical to the one to be used in the animal experiments. Beam maps and depth dose were also made using TLDs. The TLDs were brought back to USAFSAM for readout and analysis.

Experimental Procedures

The WSMR LINAC is a two-section, S-band accelerator capable of producing short pulses of high-energy electrons. The average electron energy can be adjusted from 2 to 48 MeV. An electron energy of 30 MeV was selected for this experiment in order to provide sufficient beam penetration in the event that the long axis of the animal's body (estimated to be approximately 10 cm) should be parallel to the beam during exposure.

The accelerator can be operated either continuously at 10, 20, 30, 60, or 120 pulse/sec, or in the single pulse mode. The pulse width can be varied from 10 ns to 10 μs. The dose rate (or dose per pulse) can be varied by adjusting the beam current and the distance from the exit port. Silicon diodes are used for pulse monitoring, determination of pulse shape, dose, and dose-rate measurements. These diodes are calibrated against dosimeters with calibrations

traceable to the National Bureau of Standards (NBS). The diode responses are interpreted in terms of rads silicon. A computer-controlled wave-form processing system is on line at the LINAC for monitoring the diode response and accomplishing real-time data analyses. All data can be stored on tape or disk, or printed out. Figure A-1 is a sample printout of the diode response during one of the phantom exposures.

The LINAC beam is directed into a rectangular test cell approximately 6 m wide, 8 m long, and 6 m high. A three-axis table for supporting samples and test equipment is located in front of the beam port of the exposure cell. The table can be moved longitudinally, vertically, and horizontally--either locally from inside the cell, or remotely from the LINAC console. Active monitoring of an experiment is accomplished by signal cables, run from the exposure cell table through underfloor conduits to a screened instrument room.

The phantoms used were Plexiglas cylinders, 16 cm long by 5 cm diameter, filled with water. A 6-mm i.d. Plexiglas tube on the center axis of the cylinder served for the siting of the midline dosimeters. Plexiglas spacers were inserted between the dosimeters to provide a uniform scattering medium. The exposure chamber was constructed of Plexiglas walls approximately 5 mm thick. The dimensions of the chamber were 20 cm (vertical) x 20 cm (horizontal) x 10 cm (depth). Shown in Figure A-2, an overhead view illustrating the phantom and chamber exposure configurations, are the locations of the TLDs and the WSMR diode monitor.

Harshaw (Harshaw Chemical Co., Crystal and Electronic Products, Solon, Ohio) type 700LiF power TLDs (Lot No. 1-0L-1) were used in the phantom measurements. The phantom midline dosimeters were encapsulated in #5 gelatin capsules. The front of box, and the anterior and posterior TLDs were encapsulated in polyethylene bags (4-mil wall thickness), approximately 1 cm^2 in area.

The beam maps were accomplished using Harshaw CaF_2 thin chip TLDs, arrayed in a cardboard grid at 2-cm intervals. For the exposures, the cardboard grid was mounted on the exterior front face (beam side) of the exposure chamber. The chips were also encapsulated in polyethylene bags to facilitate labeling and mounting on the grid.

The depth dose measurements were made with EG&G (Electro-Optics Div., 35 Congress St., Salem, Mass.) type 7 LiF minirod TLDs in a Plexiglas slab phantom, 15 cm wide by 15 cm deep by 12.5 cm thick. The minirods were arrayed in small holes, at varying depths, in a narrow v-shaped pattern in the center section of the slab.

All of the TLDs were read out on a Harshaw Model 2000 Thermoluminescence Dosimeter System at the USAF School of Aerospace Medicine (USAFSAM). The total integrated light output expressed in nanocoulombs of photomultiplier output was used as the dosimeter response. Electron doses in rads tissue were assigned to the dosimeters exposed at WSMR by means of comparison with calibrated sets of TLDs from the same batch or lot which had been exposed to Cobalt-60 gamma rays at USAFSAM. The gamma source was an Atomic Energy of Canada, Ltd. (AECL) Eldorado 78 Cobalt-60 unit whose output had been measured with ionization chambers with calibration factors directly traceable to NBS.

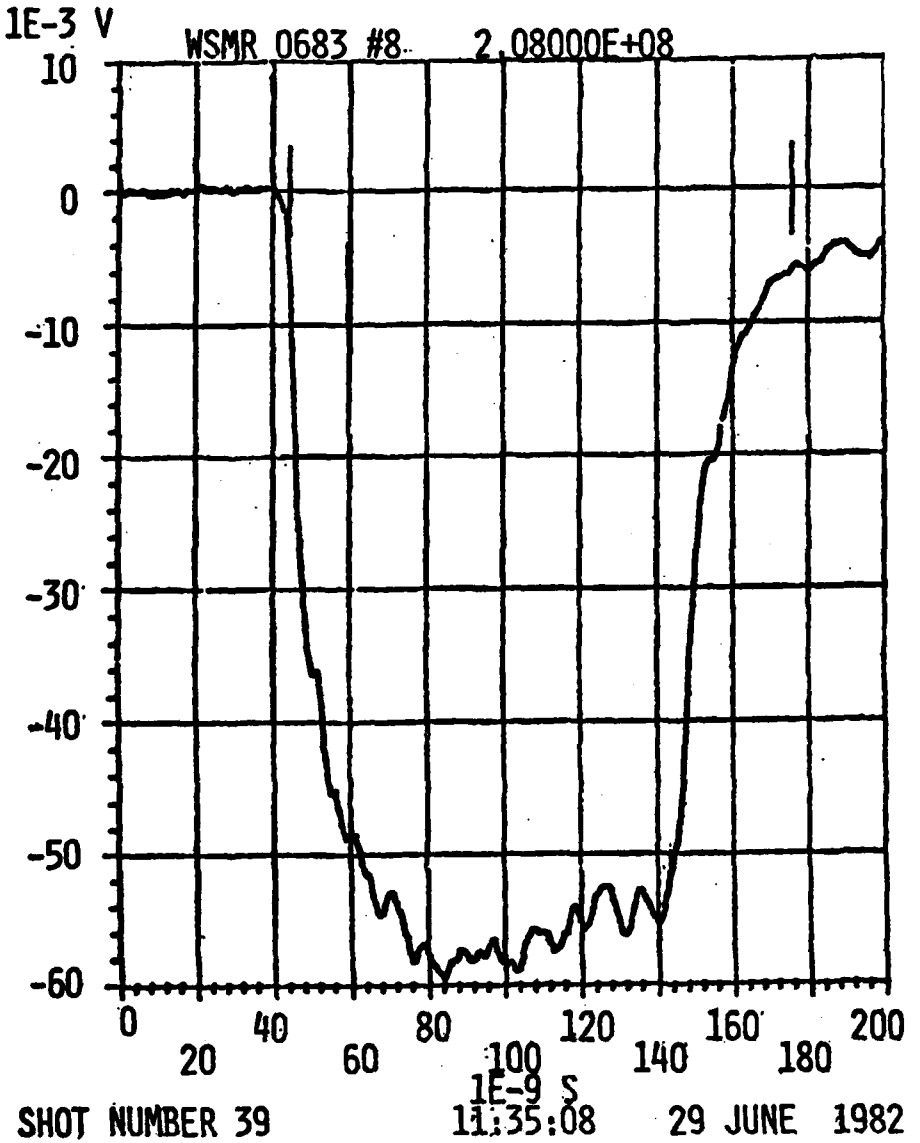

PEAK VOLTAGE
-59.5996 MILLIVOLTS

AVERAGE VOLTAGE
-44.3618 MILLIVOLTS

AREA BETWEEN TICKS
-5.83765 NANOVOLT-SEC

TOTAL DOSE
1.21423 RAD(SI)

FWHM PULSE WIDTH
101.787 NANOSEC

DOSE RATE
1.19291E+07 RAD(SI)/S

Figure A-1. Diode response at 1.0 μs pulse width, 100 rad (Si) per pulse. (Computer printout)

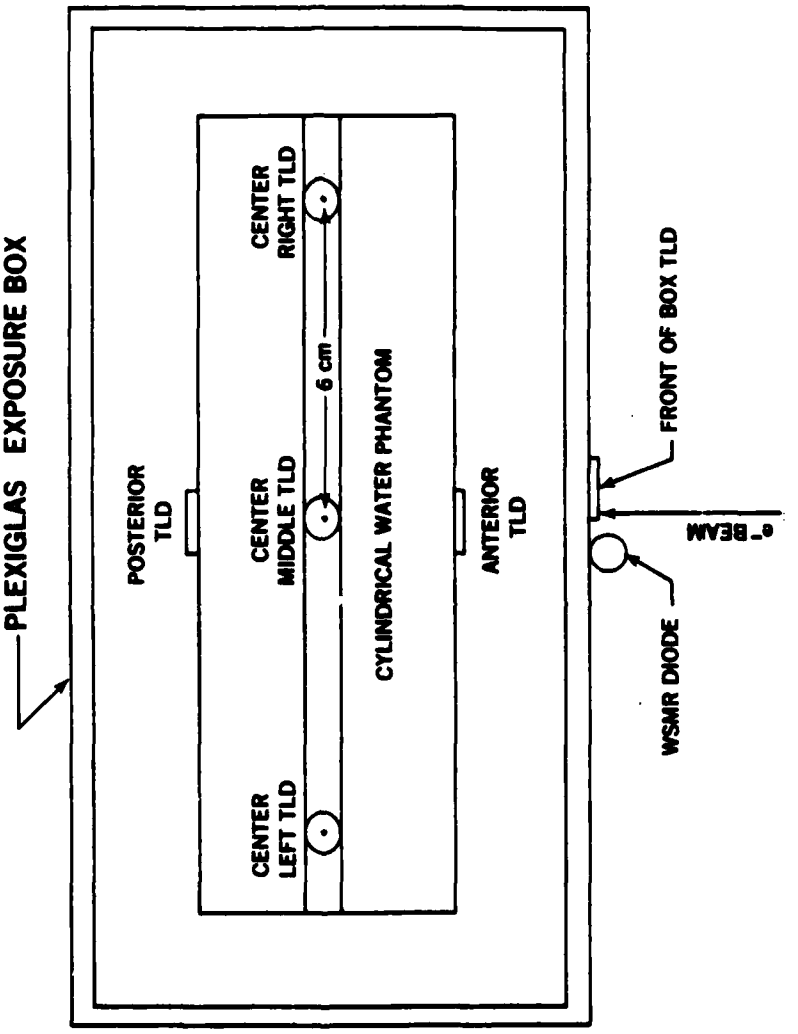

Figure A-2. Dosimeter phantom, and chamber exposure configurations (overhead view).
TLD = Thermoluminescent dosimeter.

--APPENDIX A--

The LiF powder gamma calibrations were performed in air. The powder was encapsulated in #5 gelatin capsules which, in turn, were placed in 0.5 g/cm^2 wall-thickness Plexiglas tubes to achieve dose equilibrium during the gamma exposure. A roentgen-to-rad conversion factor of 0.94 was used to convert the "in air" gamma exposures in roentgens-to-rads tissue.

The LiF minirods and CaF_2 chips were calibrated with Cobalt-60 gamma rays by exposure in a 12.5 in. thick slab phantom at a depth of 0.5 g/cm^2. A back-scatter factor of 1.08 for the 30 X 30 cm exposure field and a roentgen-to-rad tissue conversion factor of 0.94 were used to convert the gamma exposure in roentgens-to-rads tissue.

Experimental Dosimetry Results

The pulse-width dose-per-pulse combinations used in the phantom exposures have already been listed. The TLD results in rads tissue for the phantom exposures are listed in Table A-1. In general, the front of the box and phantom midline TLDs agree with the programmed dose to within ±15%, with the exception of: phantom No. 1, at 20 ns where the TLD doses are 30% to 40% too high; and phantom No. 8, where the phantom center middle, anterior, and posterior doses are 30% to 40% too low. The high dose at 20 ns at the beam center is corroborated in Table A-2, in which are listed the TLD data for the field maps and the depth dose phantom.

The phantom center dose distributions in phantoms No. 6 (1 μs, 100 rad/pulse) and No. 7 (10 μs,500 rad/pulse) indicate a significant fall off of electron dose from beam center due to inadequate beam size. This indication is corroborated by the 500 rad/pulse beam map (Fig. A-3). The 500-rad/pulse point was subsequently deleted in the July experiments. Repetition of the phantom exposures at 10 μs and 1 μs,100 rad/pulse (Phantoms A and B), performed under better exposure configurations in July, indicate a marked improvement in dose uniformity across the phantom. Figure A-4 illustrates the beam map obtained at a larger distance with 20 ns, 1 rad/pulse, 100 total pulses. The field uniformity appears to be more than adequate at this distance. The numbers listed in Figures A-3 and A-4 represent the TLD dose values in rads tissue, and the curves represent estimated percentile isodose lines. A beam map made in July at 10 μs, 100 rad/pulse, indicated exposure uniformity within 80% of the midfield value over the dimensions of the exposure box.

--APPENDIX A--

TABLE A-1. DOSIMETRIC RESULTS OF PHANTOM TLD MEASUREMENTS IN RADS TISSUE ON WHITE SANDS MISSILE RANGE LINEAR ELECTRON ACCELERATOR, 3 MAY 1982 AND 2 JULY 1982

Center middle	Center right	Center left	Front of box	Phantom anterior	Phantom posterior
1) Phantom #1: 20 ns, 1 rad/pulse, 100 pulses					
139.3	139.9	136.8	133.0	137.3	140.0
2) Phantom #2: 100 ns, 1 rad/pulse, 100 pulses					
104.2	104.7	108.6	104.3	112.3	116.2
3) Phantom #3: 100 ns, 10 rad/pulse, 10 pulses					
106.8	109.0	108.5	108.0	105.8	116.3
4) Phantom #4: 1 µs, 1 rad/pulse, 100 pulses					
98.6	108.2	105.0	-	103.6	111.4
5) Phantom #5: 1 µs, 10 rad/pulse, 10 pulses					
91.4	101.4	95.4	91.6	98.8	97.7
6) Phantom #6: 1 µs, 100 rad/pulse, 10 pulses					
925.0	829.4	676.6	903.2	907.0	942.8
7) Phantom #7: 10 µs, 500 rad/pulse, 1 pulse					
438.8	434.8	390.0	436.3	489.9	448.1
8) Phantom #8: 10 µs, 100 rad/pulse, 1 pulse					
63.8	84.4	89.5	80.7	68.5	69.5
9) Phantom #9: 10 µs, 10 rad/pulse, 10 pulses					
111.4	111.6	107.0	101.8	97.4	114.8
10) Phantom #10: 10 µs, 1 rad/pulse, 100 pulses					
94.9	113.5	98.0	100.3	89.2	-
11) Phantom A: 10 µs, 100 rad/pulse, 1 pulse[a]					
83.5	84.4	84.1	90.2	91.8	78.5
12) Phantom B: 1 µs, 100 rad/pulse, 1 pulse[a]					
84.9	78.4	81.1	97.2	121.9	83.5

[a] 2 July 1982.
TLD = thermoluminescent dosimeter; WSMR = White Sands Missile Range; and LINAC = linear electron accelerator.

--APPENDIX A--

TABLE A-2. DOSIMETRIC RESULTS OF MAP AND DEPTH DOSE TLD MEASUREMENTS IN RADS TISSUE

1) Beam map, 20 ns, 1 rad/pulse, 100 pulses

LiF powder center dose: 129.0

CaF_2 chip " " : 135.6

2) Beam map, 10 μs, 500 rad/pulse, 1 pulse

LiF powder center dose: 459.0

CaF_2 chip " " : 472.8

3) Slab phantom (depth dose), 10 μs, 1 rad/pulse, 100 pulses

LiF powder, front of box dose: 90.2 rad

LiF powder anterior of slab: 98.4 rad

4) Beam map, 10 μs, 100 rad/pulse, 1 pulse[a]

LiF powder center dose: 80.1 rad

CaF_2 chip center dose: 87.2 rad

---

[a] 2 July 1982
TLD = thermoluminescent dosimeter

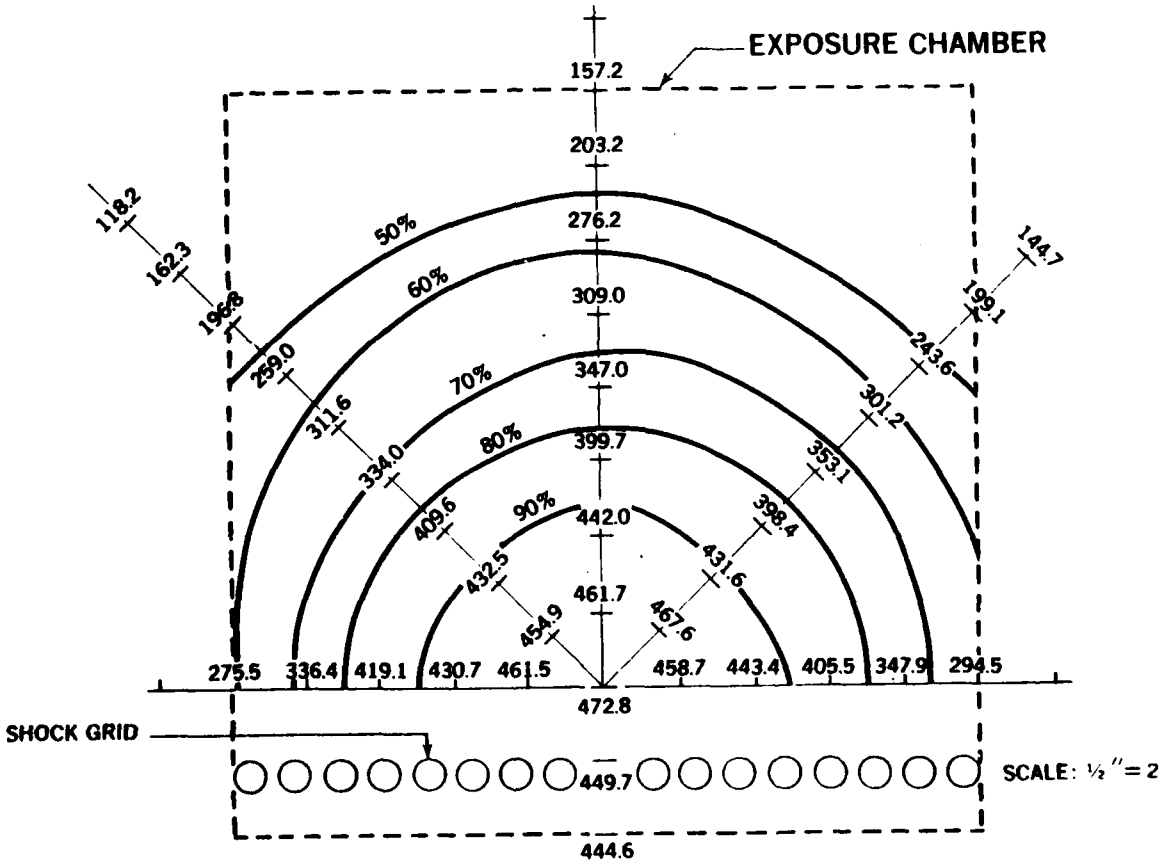

Figure A-3. Beam map: Front of chamber at 10-μs pulse width, 500 rads/pulse, one pulse.

--APPENDIX A--

Illustrated in Figure A-5 is the depth dose distribution measured with the LiF minirods in the slab phantom. The electron range is obviously more than adequate to irradiate a 10-in.-long rodent. From the measured practical range R_p (13.7 cm in Lucite, 16.4 cm in water), the electron energy was estimated to be approximately 31 MeV when published empirically derived electron range-energy equations were used (1,2). The dose contribution from X-ray production appears to be quite small, less than 4%.

In Table A-3, the results of the WSMR diode in rads silicon are compared with the TLD dose values in rads tissue obtained at the front of the box (next to the diode) and at the phantom center. Based on collision-stopping power data for 30 MeV electrons (3), we anticipated that the dose in tissue rads would be 10%-15% higher than the silicon dose. The data did not corroborate this anticipated dose. Experimental dosimetry data with TLD materials indicate a possible 5% decrease in sensitivity per rad for high energy electrons and photons when compared to Co-60 gamma rays (4)--a finding which could account for a part of this discrepancy. Based on the comparative data in Table A-3 (in the text) between the diode and the adjacent box TLD, the average TLD dose in rads tissue is about 95% of the rads silicon dose. Unfortunately, printouts of the WSMR diode doses were not obtained for all the phantom data. More data are needed to better establish the ratio between the WSMR rad silicon dose and the TLD rad tissue dose.

Discussion

The dosimetric data indicated that the WSMR LINAC was capable of delivering the requisite pulse widths and doses per pulse for this experiment, with the exception of the 500 rads/pulse, 10 μs point, which was subsequently deleted from the proposed exposure series. Increasing the exposure distance and beam current improved the exposure uniformity at the 1 μs and 10 μs, 100 rad/pulse exposure configurations in the July exposure series.

Comparative dosimetry data between the TLDs and the WSMR diode monitor indicated the diode monitor dosage in rads silicon was sufficiently close enough to the rad tissue dose to allow use of the silicon diode as the primary dose monitor for the animal exposures. Depth dose data obtained with the TLDs also indicated that the electron energy, estimated to be about 31 MeV, was adequate to penetrate the entire animal regardless of its orientation.

Operationally speaking, the WSMR LINAC facility proved to be more than adequate. The on-line computer beam control and monitoring system and the remotely operated table reduced configuration changeover time to a minimum. Little technical difficulty was encountered in accomplishing the primary experimental objectives.

--APPENDIX A--

References

1. Attix, F. H., W. C. Roesch, and E. Tochlin (eds.). Radiation dosimetry, vol. 3, ch. 19, pp. 98-100. New York and London: Academic Press, 1969.

2. Subcommittee on Radiation Dosimetry, American Association of Physicists in Medicine. Protocol for dosimetry of high energy electrons. Phys Med Biol 11 (4): 505-520 (1966).

3. Berger, M. J., and S. M. Seltzer. Additional stopping power and range tables for protons, mesons and electrons. NASA SP-3036, 1966.

4. Oberhofer, M., and A. Scharman (eds.). Applied thermoluminescence dosimetry, ch. 14, pp. 276-277. Bristol, U.K.: Adam Hilger, Ltd., 1981.

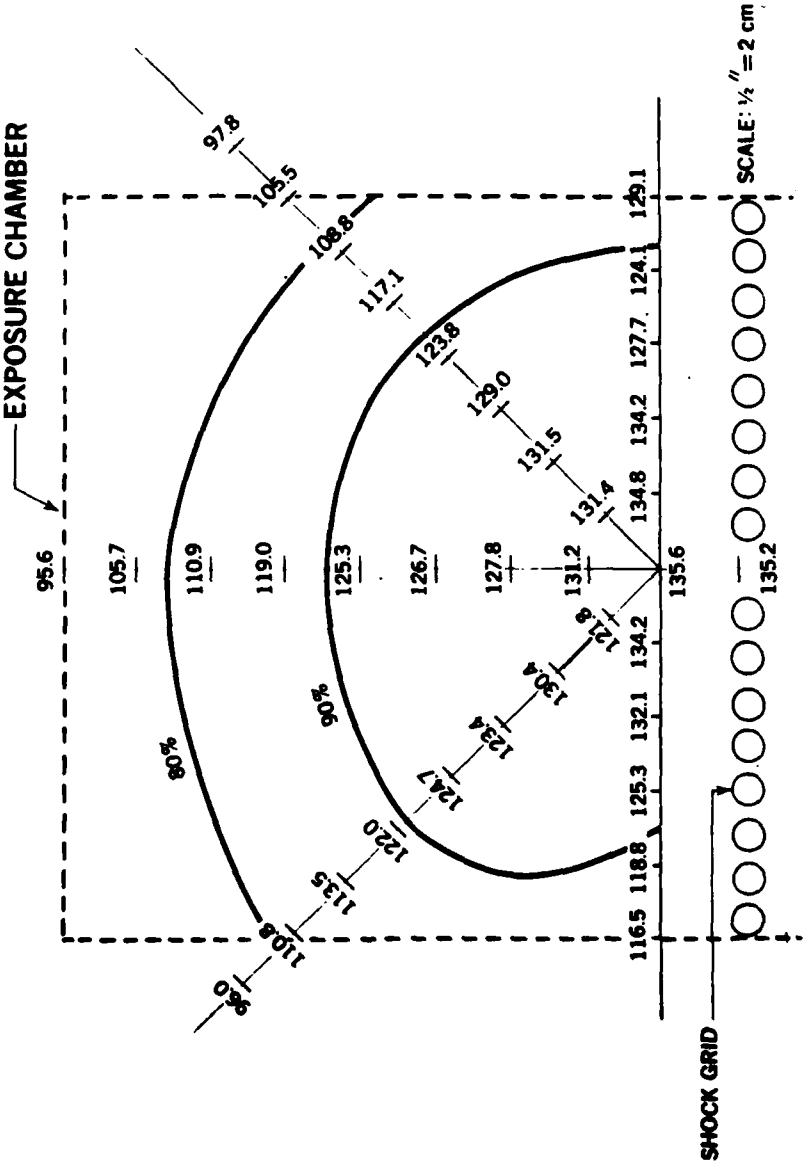

Figure A-4. Beam map: Front of chamber at 20 ns, 1 rad/pulse, 100 pulses

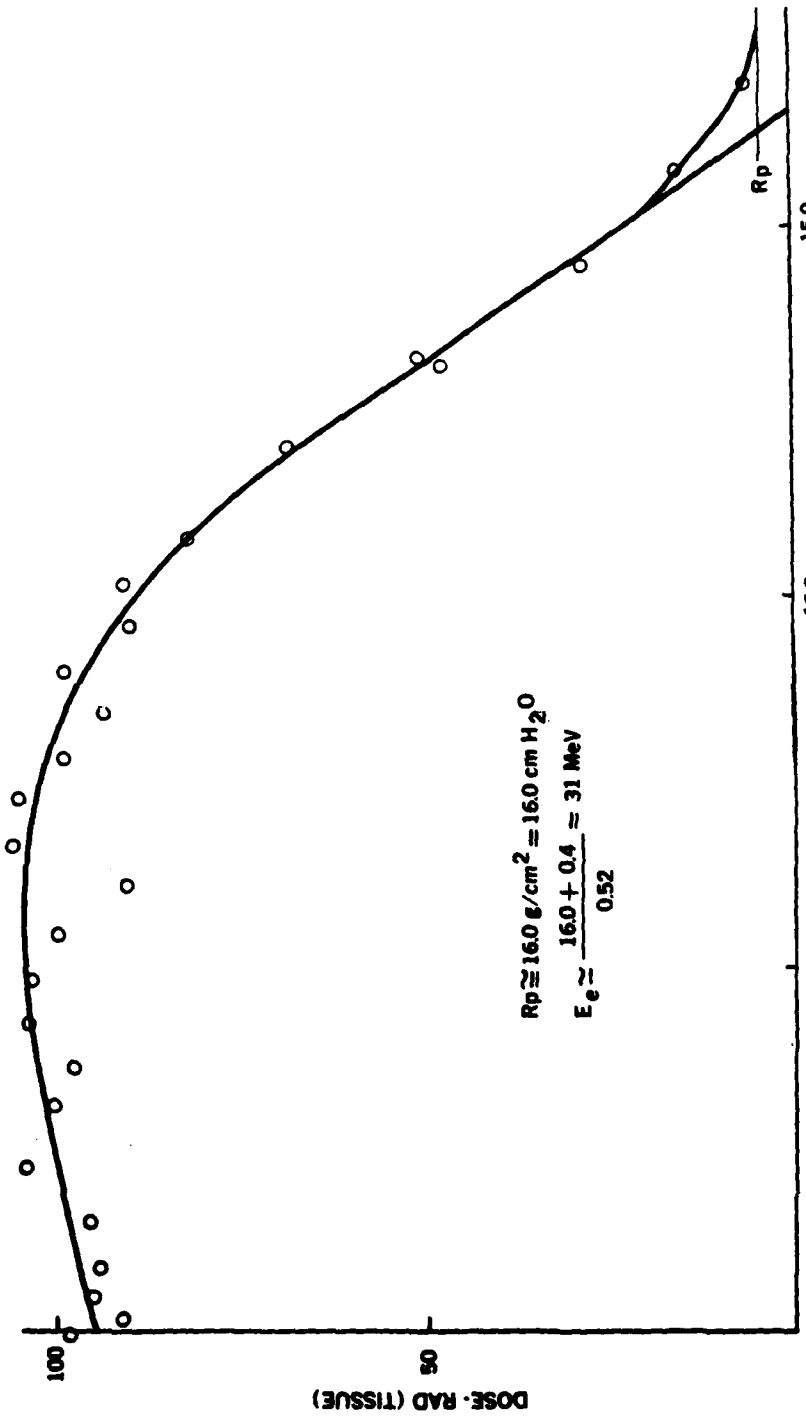

Figure A-5. Depth dose distribution measured in Plexiglas phantom at 10-μs pulse width, 1 rad/pulse, 100 pulses.

TABLE A-3. DOSE PER PULSE, WHITE SANDS MISSILE RANGE DIODE IN RADS SILICON VS. USAFSAM TLDS IN RAD TISSUE

Configuration	WSMR diode	Front of box TLD	Phantom center middle TLD
Phantom #1 20 ns 1 rad/pulse, 100 pulses	1.17	1.33 (1.14)[a]	1.39 (1.19)[a]
Phantom #2 100 ns 1 rad/pulse, 100 pulses	1.09	1.04 (0.95)	1.04 (0.95)
Phantom #6 1 μs 100 rad/pulse 10 pulses	107.0	90.3 (0.84)	92.5 (0.86)
Phantom #7 10 μs 500 rad /pulse 1 pulse	540.7	436.3 (0.81)	438.8 (0.81)
Phantom #8 10 μs 100 rad/pulse 1 pulse	84.5	80.7 (0.96)	63.8 (0.76)
Phantom #9 10 μs 10 rad/pulse 10 pulses	11.3	10.2 (0.90)	11.1 (0.98)
Phantom #10 10 μs 1 rad/pulse 100 pulses	1.04	1.00 (0.96)	0.95 (0.91)
Beam Map 10 μs 500 rad/pulse 1 pulse	382	466 (1.21)	
Beam Map[b] 10 μs 100 rad/pulse 1 pulse	101.6	80.1 (0.79)	
Phantom A[b] 10 μs 100 rad/pulse 1 pulse	99.8	90.2 (0.90)	83.5 (0.84)
Phantom B[b] 1 μs 100 rad/pulse 1 pulse	116.2	97.2 (0.84)	84.9 (0.73)
AVERAGE DOSE RATIO: (TLD rads tissue/diode rads Si)		0.94(±0.13 SD)	0.89(±0.14 SD)

[a]The numbers in parentheses are the ratios of the TLD (thermoluminescent dosimeter) dose in rad tissue to diode dose in rad silicon.

[b]Exposed 2 July 1982.

APPENDIX B:

STATISTICAL ANALYSES

Methods and Results

The main analysis was a multiple linear regression. The dependent variable consisted of the relative latencies T' - T for Groups 2 through 12, and the independent variables were $\log_{10}$ (dose) and the product $\log_{10}$ (dose) X $\log_{10}$ (dose-rate). A summary of the regression analysis is shown in Tables B-1 and B-2. These two independent variables were selected after all possible regressions were computed for up to three predictors chosen from among $\log_{10}$ (dose), $\log_{10}$ (dose-rate), $\log_{10}$ (pulse width), their squares, and the pair-wise cross products.

Preliminary summaries of the data from Group 2 through 12 revealed that the within-group distributions of values for T' - T were frequently biomodal. Concern, with how this finding might affect the validity of conclusions based on the main analysis, led to several reanalyses by alternate methods. One of these methods involved ranking all the T' - T responses from 1 to 143, and then recomputing all the possible regressions with ranks as the dependent variable to ascertain if the same predictors would still be selected as "best." A second approach was to assign the T' - T values to one of three categories (<2, $<2 \leq T' - T \leq 10$, >10) and to fit various models using the generalized least squares analysis described by Grizzle, Starmer, and Koch (1). This approach was implemented by the SAS Institute's FUNCAT procedure, with various subsets of the predictor variables inserted as quantitative columns of the design matrix X (2). The outcome of these additional analyses was to confirm the conclusion, from the main analysis, that a significant ($P<.05$) interaction occurred between dose and dose rate on the response T' - T.

The one reanalysis which gave somewhat different results was a multiple linear regression, using the group medians as a dependent variable and using the same regressors as before. The only statistically significant predictor was ($\log_{10}$ (dose)). Although an analysis of medians sometimes is appealing in cases where non-normal data are present, in this case the results based on means were more consistent with both intuition and the other analyses.

References

1. Grizzle, J. E., C. F. Starmer, and G. G. Koch. Analysis of categorical data by linear models. Biometrics 25:489-504 (1969).

2. SAS User's Guide, 1979 ed. SAS Institute, Inc., Raleigh, N. C. 27605.

--APPENDIX B--

TABLE B-1. ANALYSES OF VARIANCE AND SUMMARY STATISTICS FOR MULTIPLE LINEAR REGRESSION TO PREDICT MEAN (T' - T) DIFFERENCE FROM LOG_{10} (DOSE) AND (LOG_{10} (DOSE))·(LOG_{10} (DOSE RATE))

Source	df	SS	MS	F	P
Regression	2	8299.65	4149.83	4.67	0.011
Log_{10} (Dose)	1	4822.20	4822.20	5.43	0.021
(Log_{10}(Dose))·(log_{10} (Dose rate))	1	5991.09	5991.09	6.75	0.010
Lack of fit	8	7714.03	964.25	1.09	0.374
Error	132	117172.85	887.67		
Total	142	133186.53			

TABLE B-2. CELL VALUES ARE GROUP NUMBERS, OBSERVED CELL MEANS, AND PREDICTED VALUES (=14.52 - 36.75 LOG_{10} (DOSE) + 6.13 LOG_{10} (DOSE) LOG_{10} (DOSE RATE)·LOG_{10}DOSE RATE

Group No.	Log_{10} (dose) -1	0	1	2
8			12 24.5 (26.8)	9 31.7 (39.1)
7		11 20.6 (14.5)	8 23.0 (20.7)	5 40.8 (26.8)
6	10 14.3 (14.5)	7 2.9 (14.5)	4 4.1 (14.6)	
5	6 22.5 (20.6)	3 21.2 (14.5)		
4	2 27.7 (26.8)			

E
F
5